Idealizing Quasi-Axisymmetric 3D Geometries to 2D-Axisymmetric Finite Element Models

Jorge Camacho Casero , Trevor T. Robinson[1] , Cecil G. Armstrong[1] , Marco Geron[1]

[1]School of Mechanical and Aerospace Engineering, Queen's University Belfast,

Corresponding author: Trevor T. Robinson, t.robinson@qub.ac.uk

Abstract. This paper describes an innovative methodology which automatically creates a 2D-axisymmetric finite element (FE) model of a quasi-axisymmetric component from its 3D CAD model. The process has been implemented as a script and uses the API to a commercial FE package. The calculation of a volume shape coefficients to be applied in the non-axisymmetric regions of the FE model, to account for the fact the region is not fully axisymmetric, is also described. In the paper, the methodology is demonstrated for a rotating blade of tapered profile analyzing and comparing both stresses and displacement. Excellent results are shown.

Keywords: Idealization; quasi-axisymmetric models; axisymmetric models; finite element analysis
DOI: https://doi.org/10.14733/cadaps.2019.1020-1033

1 INTRODUCTION

There is a desire to utilize 3D Computer-Aided Design (CAD) models to represent components earlier in the design process than is currently realized. However, there is also a need to ensure that the associated analysis process is efficient, utilizing analysis models of appropriate cost and complexity for the maturity of the design. For instance, at the beginning of the development phase it can be interesting to carry out analyses of different versions of the product using simplified FE models, to select which designs are most promising based on some particular criteria (e.g. stress/deformation). Then, the analyst can refine the design and develop progressively more detailed representations, from 2D models or simplified 3D versions to fully detailed 3D models if required. However, in reality the CAD models provided to the analyst may be very complex and an idealisation step is required to make them suitable for analysis [9, 16]. In general, the main operations for geometry preparation are:

- Defeaturing: removal of geometric details which do not affect the simulation results [10]

- Geometry clean-up: removal of design features (e.g. fillets) or unintended features (e.g. slivers) due to geometric tolerances [4]

- Partitioning (divide the model): this operation is vital for the correct application of boundary conditions between regions (e.g. solid-fluid). It can also be necessary to differentiate between the different materials in a component or decomposing the geometry to create different types of meshes [13].

- Decomposition: decomposing complex geometries into simpler sub-regions to generate models suitable for mesh generation such as structured hex meshing or mixed-dimensional meshing [12].

- Dimensional reduction: representing models (or parts of models) with lower dimensionality [6] to create simplified, computationally efficient versions for simulation [2, 5].

Usually, idealizing a complex CAD model will require more than one of these operations, and much research has been devoted to managing and streamlining the process, e.g. [11]. The dimensional reduction step is at the core of this work. Specifically, the automatic creation of a 2D-axisymmetric FE model from the 3D CAD model of a quasi-axisymmetric component. A quasi-axisymmetric component is one where there is an obvious axis about which much of its geometry is axisymmetric, but it includes features which are not revolved around the axis. Some geometry clean-up operations are also required during the idealization process.

1.1 State of the art limitations for axisymmetric idealization

There are two major limitations in the field of axisymmetric idealization. The first relates to the lack of available functionalities in CAD systems to support the automatic generation of 2D-axisymmetric FE models from 3D quasi-axisymmetric CAD models. The most intuitive idea is to start by identifying the 2D profile of the part, including both axisymmetric and non-axisymmetric features. The next logical step would be to explore novel methods to identify relevant geometric features from the non-axisymmetric regions and map them to the 2D-axisymmetric profile to complete it.

Generating the outer 2D profiles from 3D CAD geometry is common practice in the CA/DCAM field [17], particularly in the context of mill-turning machining. A mill-turn part contains axisymmetric features (created from turning operations) and non-axisymmetric features (created by milling operations). Given a finalized part it is necessary to create "as-lathed" parts for generating manufacturing plans. As-lathed parts are intermediate work-pieces obtained after all the turning operations, on which the milling operations are performed later on, adding non-axisymmetric details. For instance, the model shown in Fig. 1 (a) is an as-lathed part obtained through turning processes. The milling operations are performed on this part to generate the finalised part is depicted in Fig. 1 (b).

(a) As-lathed part from turning operations.

(b) Finished part resultant from a turn-mill process.
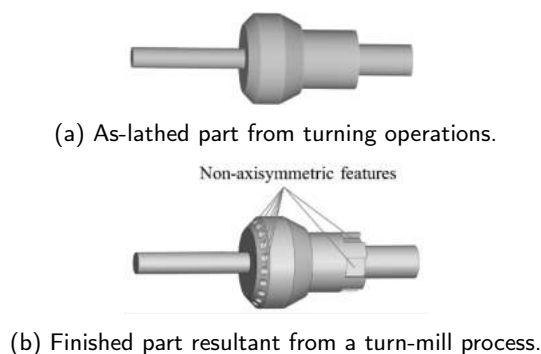
Figure 1: Figure adapted from [8]

The common approach used in the literature to generate as-lathed models consists of revolving all the faces of the finished part around the axis of revolution to fill-in the gaps between non-axisymmetric features.

Unfortunately, the revolve operation presents many important drawbacks. Wentao in [8] stated that revolve operations are computationally expensive when dealing with many 3D geometries, time consuming and potentially inaccurate. Due to these drawbacks, which were also observed over the course of this work, it was decided not to use revolve operations as part of the automatic idealisation procedures. Besides, there was also the desire to create a CAD vendor independent solution, able to produce 2D CAD models in a neutral format so they can be imported into any FE package for meshing and analysis.

The second limitation relates to the lack of investigation on simulation techniques for the axisymmetric analyses of quasi-axisymmetric models. Currently, axisymmetric analyses are mainly performed on truly axisymmetric models or on quasi-axisymmetric models, where it is assumed that the impact of the non-axisymmetric features on the analysis results is negligible and are simply ignored in the analysys (e.g. the tiny holes in Fig. 1 (b)). However, for many components the non-axisymmetric features cannot be considered negligible and must be accounted for in the axisymmetric analysis to ensure the results obtained are representative of the behaviour of the 3D component. While in Abaqus [1] a manual approach can be used to account for some simple non-axisymmetric cylindrical hole features for which the effect can be mathematically derived, to the authors' knowledge there are no published methods to automatically account for general non-axisymmetric features in an axisymmetric analysis.

This paper presents an automated idealization methodology for creating a 2D-axisymmetric FE model from the 3D CAD model of a quasi-axisymmetric component. An approach to account for non-axisymmetric features in an axisymmetric analysis based on a geometric attribute (shape coefficient) is also discussed. This coefficient is used to correct the material properties and loads on the non-axisymmetric regions of the 2D-axisymmetric FE model.

2   The Idealisation process

The idealisation methodology presented here has been implemented in two main stages: i) a software capability developed in the C# programming language for the creation of the 2D-axisymmetric profile and ii) a Python script which exploits the Abaqus Python Scripting Interface to calculate the shape coefficient from the CAD model and meshing operations. The input is a triangular facetted representation of the CAD geometry. A facetted representation was selected as the input because it can be created for all common engineering geometry types (e.g. NURBS geometry, analytic CAD geometry, meshed geometry and point clouds). The facetted representation is created by replacing each of the faces of a model by a set of triangular facets. The quickest way to achieve this is to export the geometry from the CAD system in a facetted format. VRML was the format used in this work because it is well documented and widely available, but the approach would work equally well with any triangular surface mesh/facet representation. The mesh coarseness should be selected to reflect the size of the features in the part, but increasing the number of elements will impact the processing time. One of the advantages of the VRML writers is that they use element sizes suited to the scale and curvature of the model. Note that, while it is possible to analytically compute an analytic description of an analytic shape when projected on a plane, it is not possible to do this for NURBS geometry. The different steps implemented in the process are further reported with the geometry at different stages shown in Fig. 2.

### 2.1   Step 1: Projecting face facets circumferentially onto the *r-Z* plane

The 2D axisymmetric model exists on a plane, consequentially the first step in the idealisation of the component model involves circumferentially projecting the facets representing each face onto a plane. The plane is referred to as the $r - Z$ plane where r is the radial direction and Z the axial. The circumferential projection of a face onto the $r - Z$ plane implies a $\Re^3 \rightarrow \Re^2$ transformation from the Cartesian coordinate system (x, y, z) to a new set of coordinates in (r, Z) space. Depending on the direction of the axis of revolution in the component model the specific transformation will differ, but for each facet vertex the r coordinate is the shortest distance

of the point from the axis of revolution, and the Z coordinate of the vertex remains at its current value in the axial direction. For example, assuming the axis of revolution is the z-axis, the transformation is $(x, y, z) \rightarrow (r, Z) = (\sqrt{(x^2 + y^2)}, z)$.

2.2 Step 2: Classifying faces

Once the facets representing the model faces have been projected onto the $r - Z$ plane, it is necessary to classify them, so that they can be used to describe the overall shape of the final 2D-axisymmetric model in future steps. The classifications are:

- Case 1: After the projection, the 3D face becomes a 2D degenerate face of zero area (referred to as a "mapping face" in this work). This occurs when the area of every facet representing the face becomes zero after the projection. For example, this is the case of faces F1 to F5 in Fig. 2

- Case 2: These are faces that include some facets that have non-zero area when projected circumferentially onto the $r - Z$ plane. For example, faces F6 to F9 in Fig. 2
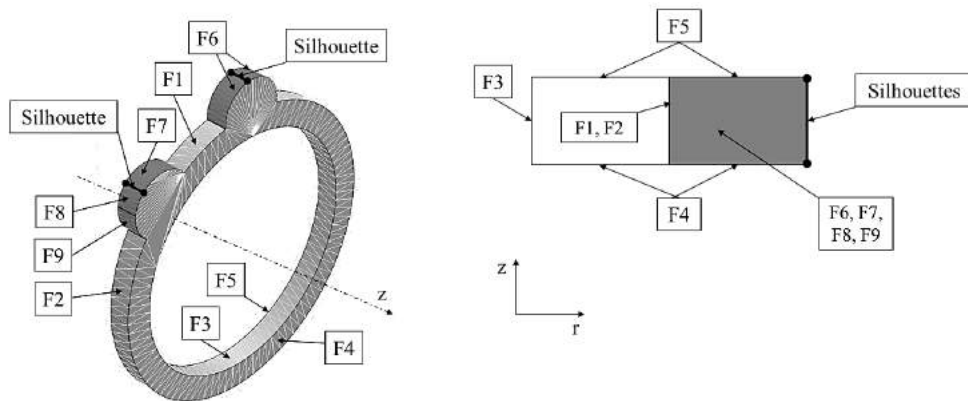
Figure 2: Key elements in the 3D model (left) and the equivalent 2D-axisymmetric profile (right).

2.3 Step 3: Identification of mapped edges

To extract a set of edges to define the axisymmetric profile of the part, the set of facets identified in step 2 as case 1 are used. As they have zero-area, these projected facets have three collinear vertices. The associated mapped edges can be identified by eliminating the intermediate vertex (or a coincident vertex), leaving only the extreme points. The mapped edges are then stored in a list called SHAPE-EDGES for use in step 5.

2.4 Step 4: Identification of silhouettes edges

Silhouette edges define another set of edges required to define the axisymmetric profile. Silhouette edges are identified as those bounding adjacent facets whose normals point in opposite directions after the projection to the $r - Z$ plane. The facet normals can be calculated by taking the vector cross product of two edges of that triangle (where the edge vectors can be computed based on the end point locations). For example, in Fig. 3 the normals of facets A and B initially point out of the body in 3D space, Fig. 3 (left), as is the standard for a CAD model. After being projected on the $r - Z$ plane, the normal of these facets point in opposite directions

(Fig. 3 (right)). Hence the edge shared by facet A and B is a silhouette edge. Note that this is not the case for adjacent facets C and D or E and F, since adjacent normals point in the same direction after the projection onto $r - Z$. Hence, they do not share a silhouette edge.
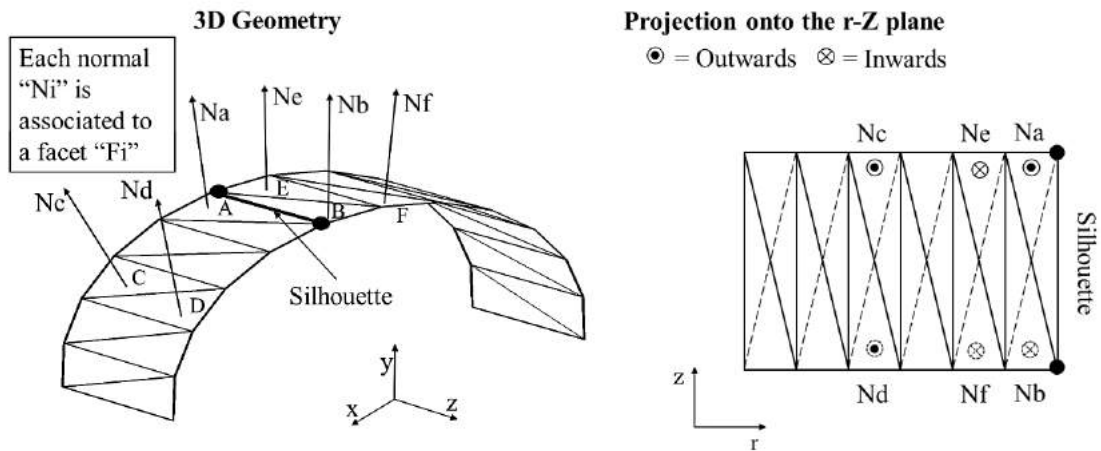
Figure 3: Silhouette curves of a 3D geometry viewed from the axis of revolution and definition of the normal of representative facets (left) and definition of a silhouette curve in the $r - Z$ plane (right).

The identified silhouette edges are added to the SHAPE-EDGES list which now contains all the necessary edges to form the 2D-axisymmetric profile. This list represents the input to step 5.

2.5   Step 5: Obtaining a raster representation of the 2D-axisymmetric profile

The set of SHAPE-EDGES is sufficient to define the overall boundaries of the 2D-axisymmetric model. However, at this stage the shape edges are not topologically connected and cannot be used directly to identify the topology of the 2D-axisymmetric model. This is due to the fact many of the edges will be redundant, because many faces will potentially have projected onto the same locations. This may mean many edges overlapping within a very small tolerance, as shown in Fig. 4 (a). The visual effect of the overlap of the edges in this figure has been magnified for illustration purposes.

In this work, rasterization strategies are used to deal with the edge redundancy issue and to generate an appropriate data representation for topology construction via contour recognition techniques (addressed in step 6). The rasterization approach consists of discretizing the $r - Z$ plane to a square grid (i.e. a raster formed by square cells Fig. 4 (b)) which the shape edges are mapped to. If a cell in the raster is intersected by one or more edges, then the cell is stored. This way many edges can be reduced to a set of unique cells, Fig. 4 (c). In this work Bresenham's line algorithm [3] was used. By applying the rasterization approach, the 2D-axisymmetric model profile is reduced to a binary structure from which the regions that form the 2D-axisymmetric model can be extracted in step 6.

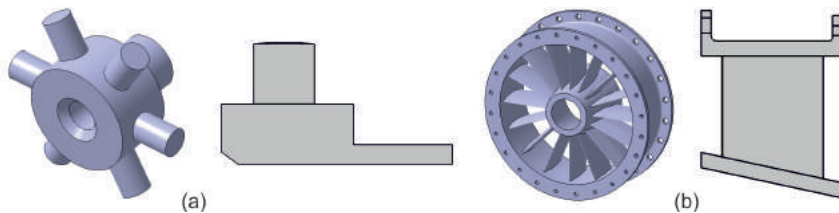## 2.6   Step 6: Building the 2D-axisymmetric model

In this work, the OpenCV image processing library (particularly the .Net wrapper EmguCV) was used to identify contours in the binary structure resulting from method 5. EmguCV contains a function for contours retrieval (findContours) based on Suzuki´s algorithm [15]. The contours detected using this function (Fig. 4 (c)) are
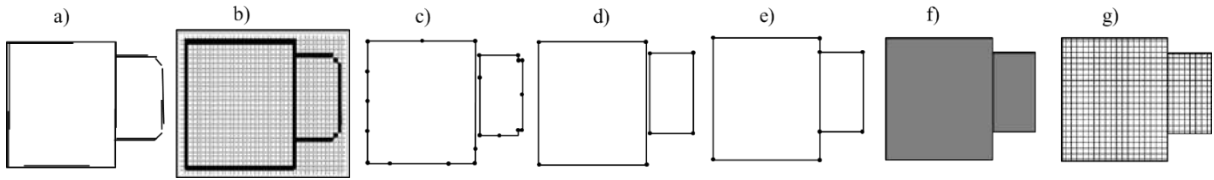
Figure 4: (a) Overlapping edges in a 2D-axisymmetric profile; (b) Overlapping edges reduced to a set of unique cells; (c) Contours detected in the binary profile; (d) Simplified contours using Douglas-Peucker algorithm; (e) Stitching of the simplified contours; (f) 2D-axisymmetric CAD model; (g) 2D-axisymmetric FE model

stored as arrays of points defining polygons. It was identified that the resultant polygons can be unnecessarily complex from a FE perspective, and require simplification to help reducing the resolution (i.e. the edges defining the polygons are much shorter than the element size). To simplify the polygons, the Douglas-Peucker algorithm [7] (function ApproxPoly in EmguCV) was used. This algorithm identifies and compresses horizontal, vertical, and diagonal segments to single entities, as illustrated in Fig. 4 (d). Typically, the simplified polygons have small gaps between them after the rasterization and simplification operations. Hence, stitching the polygons together is necessary (Fig. 4 (e)). To achieve this the "Stitch" command implemented in Abaqus/CAE is used. The resulting set of polygons represent the 2D-axisymmetric model. These polygons can be converted into a usable CAD model (Fig. 4 (f)) by writing them in a format such as STEP.

The automated idealisation result of some simple concepts are shown in Fig. 5. In each case the CAD models were created in CATIA V5 and were dimesionally reduced in under 30 seconds on a standard desktop workstation. Note that the model on the right has blades with aerofoil profiles.

Figure 5: Automated rebuild of axisymmetric shape

3 Axisymmetric FE model

3.1 Definition

The 2D-axisymmetric FE model Fig. 4 (g) is obtained by meshing the CAD model resulting from the six steps described in section 2. In this work the creation of the FE model was automated using the ABAQUS Python API. The main steps in the model creation were the automation of the creation of an axisymmetric profile and appropriate boundary conditions (e.g. $U_y = 0, R_x = 0 \, and \, R_z = 0$, where x is the axial direction and z is the radial) and the application of 2D axisymmetric elements (e.g. CAX6M) in the different sub-regions of the model. The conversion of a 3D quasi-axisymmetric model to its equivalent 2D-axisymmetric representation results in a loss of the geometric information contained in the circumferential dimension. In order to ensure the physical relevance of the 2D-axisymmetric model with respect to the original 3D model, the information loss

must be compensated. A physically straightforward way to account for this, is to modify the 2D-axisymmetric FE model with a shape coefficient applied to the material properties.

For this purpose, the "Volume Fraction" coefficient (K_V) has been defined. This coefficient establishes for each region in the model the fraction of the volume around the axis of revolution the 3D model actually occupies. This coefficient is equal to 1 for an axisymmetric region.

3.2   Correction of material properties and loads

Correcting material properties when performing analyses using the 2D-axisymmetric model is key to obtaining physically realistic results. Obviously, the type of material properties to be corrected will depend on the type of analysis performed. In this work, this has been investigated from a mechanical analysis perspective. To understand what type of material properties must be corrected in the proposed mechanical analysis, the equations defining the behaviour of the material for the 3D and 2D axisymmetric geometries are compared.
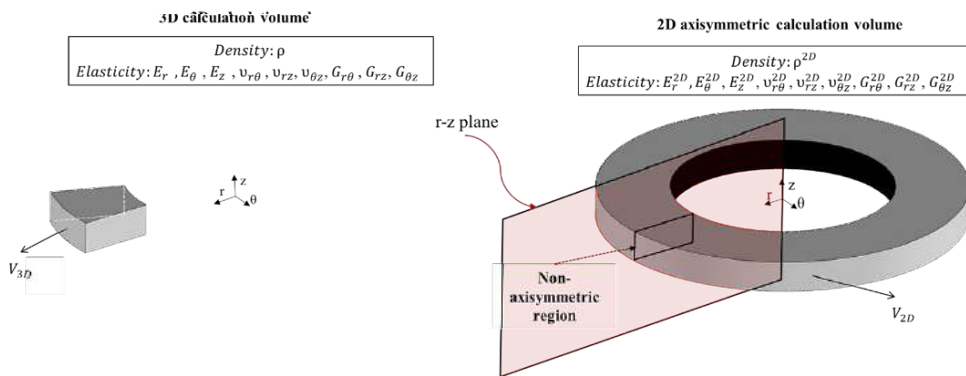
Figure 6: Non-axisymmetric calculation volumes for the 3D and the 2D-axisymmetric models

First, the two domains must be identical in terms of mass. However, since the parameter most commonly applied in FE packages is not the mass but the density, the latter is used instead. The actual mass of the 3D volume is given by the density (ρ) multiplied by the actual volume (V_{3D}). This must equal the density applied to the axisymmetric volume (ρ_{2D}) multiplied by the assumed axysymmetric volume (V_{2D}). Equating the masses on both domains gives

$$\rho V_{3D} = \rho_{2D} V_{2D} \Rightarrow \rho_{2D} = \rho \frac{V_{3D}}{V_{2D}} \tag{1}$$

where the ratio $\frac{V_{3D}}{V_{2D}}$ is precisely the volume fraction K_V. Hence, the density of the axisymmetric calculation volume must be corrected following the relationship $\rho_{2D} = \rho K_V$. Second, it must be ensured the equivalence from a loading perspective and this is assured by considering the "Strain Energy". If a perfectly elastic material is deformed, all the energy put into this deformation must be recovered by bringing the material to its initial state [14]. This energy (denoted by U) is defined by the stress and strain vectors in a generic differential volume dV through the expression

$$U = \frac{1}{2} \int_V \{\sigma\}\{\varepsilon\} dV \tag{2}$$

Finally, if Eq. 2 is written in terms of the strain vector alone and if it is considered that the 3D and the axisymmetric volume calculations must exhibit the same elastic behaviour (stress and strain) it is possible to imply that they must have the same energy strain magnitude ($U_{3D} = U_{2D}$). It is thus possible to write

$$\int_{V_{3D}} \{\varepsilon^T\}\mathbf{E}\{\varepsilon\}dV_{3D} = \int_{V_{2D}} \{\varepsilon^T\}\mathbf{E_{2D}}\{\varepsilon\}dV_{2D} \tag{3}$$

Since there is the desire to maintain an equivalence between the two domains, the strains $\{\varepsilon\}$ must be the same on both sides of Eq.3. Hence, the only term that can be used to equal the energy strain magnitudes is the material stiffness. Therefore, it can be deduced that

$$\mathbf{E}dV_{3D} = \mathbf{E_{2D}}dV_{2D} \Rightarrow \mathbf{E_{2D}} = \mathbf{E}\frac{dV_{3D}}{dV_{2D}} \tag{4}$$

where the ratio $\frac{dV_{3D}}{dV_{2D}}$ is precisely the volume fraction (K_V). Therefore, to make the axisymmetric analysis equivalent to the 3D analysis, each of the elements of its elasticity matrix must be multiplied by the volume fraction K_V, giving

$$\mathbf{E_{2D}} = K_V\mathbf{E} \tag{5}$$

From a physical point of view, reducing the Young´s modulus in the radial and longitudinal directions corrects stiffness effects in the axisymmetric plane. Fig. 6 summarises the material properties to be edited when using a 2D axisymmetric model to represent a non-axisymmetric feature. If isotropy in the $r - Z$ plane is assumed then E_r^{2D} equals E_z^{2D}. In a quasi-axisymmetric model of structures such as turbines or turbine casings, the non-axisymmetric features usually only occupy a small fraction of the volume. This implies that, in these features, any normal or shear stress with a component in the hoop direction are negligible. A convenient way of enforcing this condition in a quasi-axisymmetric model is to specify material moduli which are negligible in the hoop (θ) direction, i.e. to use an anisotropic material model where the properties in the r-Z plane are given by Eq. 5, but the modulus in the θ direction is negligible. An example is given in Table 1.

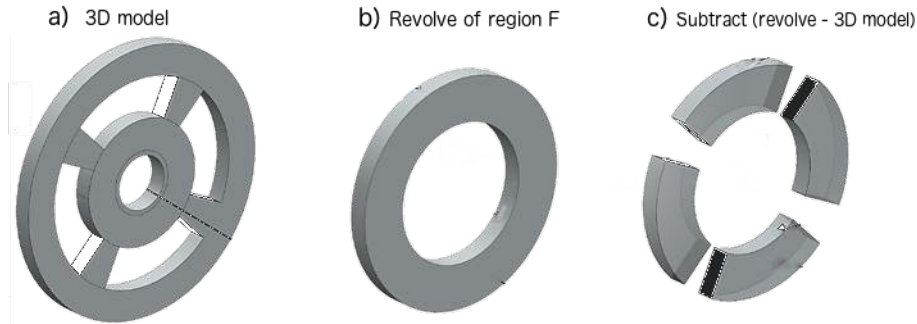## 3.3   Automatic calculation of the shape coefficients

The process has been implemented in Abaqus by inputting the 3D and the 2D axisymmetric CAD models followed by the creation of two bodies named "Revolve" and "Subtract". These are depicted in Fig. 7 (b) and Fig. 7 (c) respectively for the input model in Fig. 7 (a).

- "Revolve" represents the totality of the material around the circumference and is generated by revolving the non-axisymmetric region (referred to as F) around the axis of revolution.

- Subtract represents the material which should not be represented in the 2D axisymmetric model, and is generated by the Boolean subtraction of the original 3D model from "Revolve".

The calculation of the Volume Fraction (K_V) is straight forward. It only requires the volumes of the two counter-parts, denoted by "Vol (Revolve)" and "Vol (Subtract)" respectively, as

$$K_v = \frac{Vol\,(Revove) - Vol\,(Subtract)}{Vol\,(Revolve)} \tag{6}$$

It is obvious from this equation that a Volume Fraction value ranges from zero to one. Volume fractions close to zero indicate very little material around the circumference. Conversely, if the Volume Fraction reaches unity the geometry is fully axisymmetric (and the application of any of the shape coefficients in not required).

Figure 7: (a) 3D Model, (b) Revolve and (c) subtract counter-parts for the calculation of the shape coefficients

4 Validation

4.1 Test case definition

To validate the proposed methodology a rotating blade of tapered profile is analysed. The radial stresses and displacement resultant from both the 3D model (Set-up A), the generated 2D-axisymmetric model with corrected properties (Set-up B corr) and the analytical model are compared.

The 3D model is depicted in Fig. 8 and consists of a shaft with 20 tapered blades occupying 2% of the volume at all radii, consequently the volume fraction K_V is equal to 0.02 for entire non-axisymmetric region. The geometry studied is cyclically symmetrical about the axis of revolution; hence, analysing just one sector is sufficient to obtain representative results for the entire model. Stresses and displacements acting along the radial direction caused by a centrifugal body force are evaluated in this example. It is assumed that the blade is rotating with an angular velocity $\omega = 250\ rad/s$. The isotropic material properties for the 3D model and the corrected properties for the axisymmetric analysis are reported in table 1.

	Density $[Kgm^{-3}]$	E1 $[MPa]$	E2 $[MPa]$	E3 $[MPa]$	G12 $[MPa]$	G13 $[MPa]$	G23 $[MPa]$
Properties	7700	200000	200000	200000	77000	77000	77000
Corrected Properties	154	4000	4000	4E-3	1538.5	2E-3	2E-3

Table 1: Material properties and corrected material properties

The material properties have been corrected following the logic presented in [1]:

- The density of the non-axisymmetric region is multiplied by the volume fraction to make the mass of the axisymmetric calculation volume equal to the mass of the blades.

- The effective in-plane Young´s modulus, E_r^{2D} and E_z^{2D}, are obtained by multiplying the respective radial and longitudinal Young´s moduli, E_r and E_z ,by the volume fraction thus $E_r^{2D} = E_z^{2D} = E^{2D} = K_V E$. Reducing the Young´s modulus in the radial and longitudinal directions aims to correct the stiffness. The modulus in the circumferential direction, must also be reduced to account for the fact that there are

"air" gaps between the blades. This value must be very small since there no stiffness in the circumferential direction and is chosen such that $\frac{E_\theta^{2D}}{E^{2D}} = 10^{-6}$ (value taken from [1] for the same material).

- The in-plane shear modulus is then calculated based on the corrected Young´s modulus following the relationship $\mathbf{G}^{2D} = \frac{\mathbf{E}^{2D}}{2(1+\nu)}$.

- The shear moduli in the 12 and 23 directions are assumed to be negligible.

The analytical expression for the stresses along the midline of the component can be divided into two different components, one for the shaft section and one for the blade.

The radial stresses for the shaft section ($0 \leq r \leq r_1$) (refer to Fig. 8) can be defined as

$$\sigma_{r_s} = A + \frac{3+\nu}{8}\rho\omega^2\left(r_1^2 - r^2\right) \tag{7}$$

where $\nu = 0.3$ is the Poisson's ratio, $\omega = 250rad/s$ is the angular velocity, the density ρ is given in table 1 and A represents the stresses at the blade-shaft interface. A can be evaluated as:

$$A = \frac{m_{blade} \cdot \omega^2 \cdot COG}{\pi r_1^2 t} \tag{8}$$

where m_{blade} is the mass of the blade, t its thickness and COG the centre of gravity of the blade.

The radial stresses along the midline of the tapered blade ($r_1 \leq r \leq r_2$) can be defined as:

$$\sigma_{r_b} = \rho\omega^2\left(\frac{r_2^2}{3r} - \frac{r^2}{3}\right) \tag{9}$$
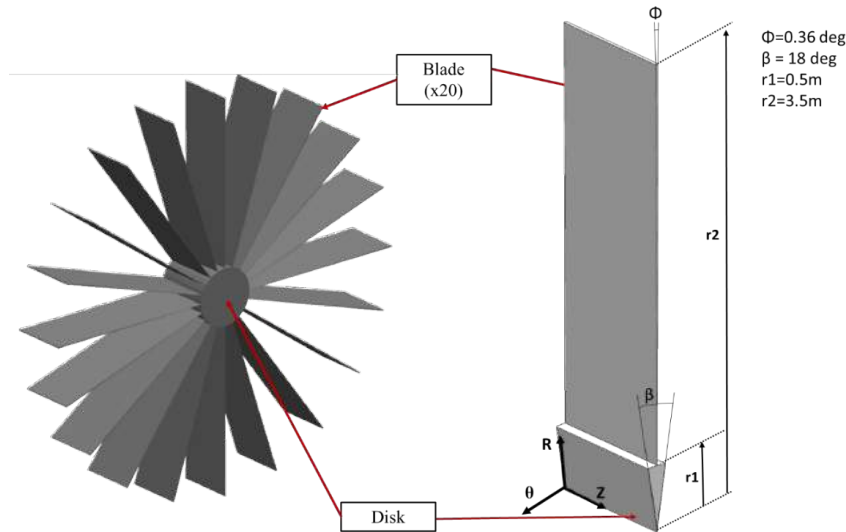
Figure 8: Shaft with 20 tapered blades uniformly distributed along the circumference and 1/20th sector of the same geometry

Both FE models have utilised quadratic elements with the same density on the plane of the blade. The two set-ups are represented respectively in Fig. 9 where the boundary conditions applied are also reported.
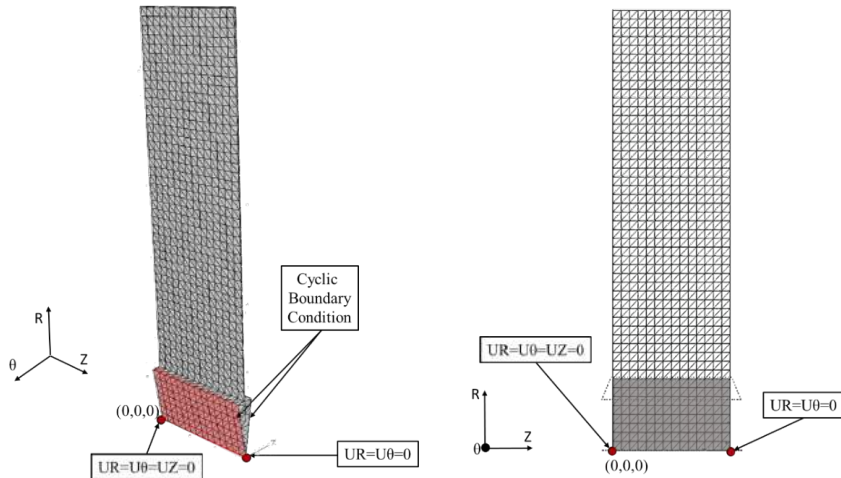
Figure 9: Analysis Set-up A (left) and Analysis Set-up B (right)

4.2 Results and discussion

Radial stress: The contour plots of the radial stress for the 3D section (Set-up A) and the corrected 2D axisymmetric (Set-up B Corr) are shown in Fig. 10 left and right respectively. From the figure it is visible that the results obtained from the two different set-ups are similar.
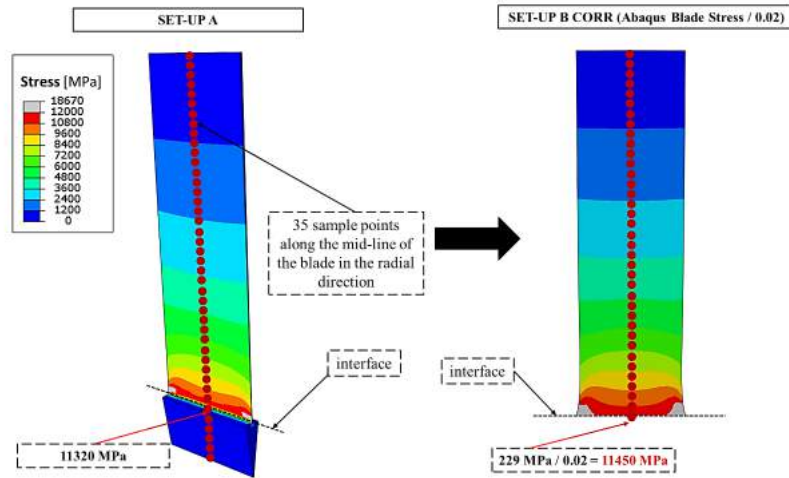
Figure 10: Stress contour plots for Set-up A (left) and Set-up B (right) where the stress on the blade is corrected by the volume fraction

To carry on a quantitative analysis of the behaviour of the stress, 35 points radially distributed along the

midline of the shaft and blade have been taken from both set-ups (red points in Fig. 10). Their values have been plotted in Fig. 11 and compared with the analytical solution obtained from Eq. 7 and 9. In Fig. 11 the red triangles represent the stress values of set-up A, the black crosses shows the stress values of Set-up B and the green line represents the analytical solution. Note that the first $500mm$ is the shaft, while the range from $500mm$ to $3500mm$ is the blade.
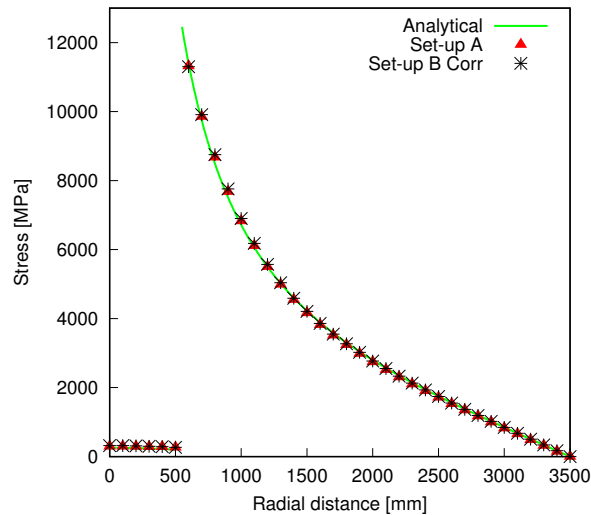
Figure 11: Stress along the radial direction for Set-up A and Set-up B Corr and analytic solution

The maximum radial stress along the midline of the blade is at the interface between the disk and the blade. At this particular point, Abaqus provided a stress of 11320 MPa for set-up A and 11450 MPa for set-up B. From the interface on, the radial stress decreases progressively along the length of the blade. To provide a further quantitative insight of the relative differences (deviation) between the two set-ups, the stress and displacements at the sample points obtained on both set-ups are mapped against each other to outline the relative difference (see distance to the line of slope equal to one) between both analyses. Fig. 12 and Fig. 13 show the differences between both set-ups in terms of stress and displacement respectively.

The maximum deviations occur at the interface between shaft and blade. In the middle of the interface (where the red point is) the deviation is circa 1.5% for the stress and 1.1% for the displacement. On the interface there are two points where the stress gets concentrated (shown grey in Fig. 12). Here the complex stress concentrations cannot be appropriately represented by the axisymmetric model which leads to higher deviations at these two points with values of 6.8% for the stress and 4.4% for the displacement. At this radius the axisymmetric model has to represent both the free surface of the shaft plus the connection of the shaft with the blade.

5 Conclusion and future work

From this work, the following conclusions can be drawn;

- An innovative methodology which automatically creates a 2D-axisymmetric model for a quasi-axisymmetric component from its 3D CAD model, in very short timescales, has been presented.
- A shape coefficient is used to correct the material properties when performing axisymmetric finite element analysis.
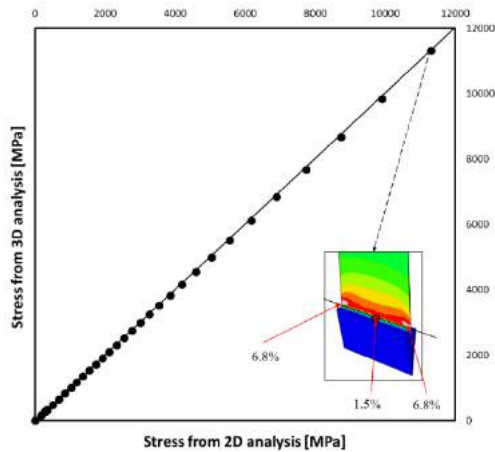
Figure 12: Relative difference between set-up A and B (stresses)
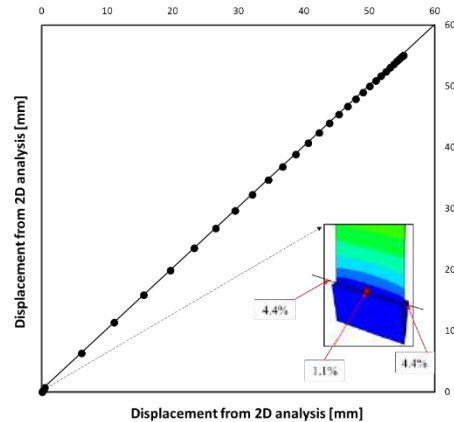
Figure 13: Relative difference between set-up A and B (displacements)

- The ensemble of idealization methodologies described have been implemented in a fully automated software prototype.

- The accuracy of this shape coefficient is tested through load analysis on a rotating blade of tapered profile.

- Accurate results are reported.

Over the course of this work, the idealisation and analysis of even seemingly complex models has required less than 5 minutes to process. In the process described above, one K_v value is calculated for each quasi-axisymmetric region in the model. This was fine for the example model because the tapered blade profile meant that the K_v value was constant across the blade, and the calculated K_v was accurate at all positions. Should the thickness of the geometric features in the axisymmetric regions not exhibit this property, then the K_v value calculated will be the average for the region. Should the average not be sufficient then the quasi-axisymmetric profiles in the 2D model can be divided into smaller regions. This will produce smaller sections, each with a K_v value averaged for the region they cover. At the highest level of granularity, the quasi-axisymmetric regions can be meshed in the 2D model, and each element treated as a separate region. This will provide the highest possible accuracy, but there will be a cost associated with its computation.

Future research will involve testing the idealisation methodologies on components from other industry sectors and investigating extension of the methodology to other Finite Element Analysis disciplines.

6   Acknowledgements

ORCID

Cecil G. Armstrong, http://orcid.org/0000-0001-8695-5016
Trevor T. Robinson, http://orcid.org/0000-0002-6595-6308
Marco Geron, http://orcid.org/0000-0003-4231-0982

REFERENCES

[1] Abaqus: Abaqus-Examples Manual, 2017. Bolted pipe Joint- section 1.1.1-3.

[2] Armstrong, C.G.: Modelling requirements for finite-element analysis. Computer-Aided Design, 26(7), 573–578, 1994. http://doi.org/10.1016/0010-4485(94)90088-4.

[3] Bresenham, J.: Bresenham's line algorithm. IBM Systems Journal, 4, 25–29, 1965.

[4] Clark, B.W.: Removing small features with real CAD operations. In Proceedings of the 16th International Meshing Roundtable, 183–198. Springer, Berlin, Heidelberg, 2007. http://doi.org/10.1007/978-3-540-75103-8_11.

[5] Donaghy, R.J.; Armstrong, C.G.; Price, M.A.: Dimensional reduction of surface models for analysis. Engineering with Computers, 16(1), 24–35, 2000. http://doi.org/10.1007/s003660050034.

[6] Donaghy, R.J.; McCune, W.; Bridgett, S.J.; Armstrong, C.G.; Robinson, D.J.; McKeag, R.M.: Dimensional reduction of analysis models. In Proceedings of the 5th International Meshing Roundtable, 307–320. Sandia National Laboratories, Pittsburg, PA, 1996.

[7] Douglas, D.H.; Peucker, T.K.: Algorithms for the reduction of the number of points required to represent a digitized line or its caricature. The Canadian Cartographer, 10, 112–122, 1973.

[8] Fu, W.; Eftekharian, A.A.; Campbell, M.I.; Kurtoglu, T.: Automatic reasoning for defining lathe operations for mill-turn parts: A tolerance based approach. Journal of Mechanical Design, 136(12), 121701–121701–10, 2014. http://doi.org/10.1115/1.4028275.

[9] Handi, M.; Aifaoui, N.; Benamara, A.: Idealisation of cad geometry using design and analysis integration features models. In International Conference of Engineering Design. Paris, France, 2007.

[10] Lee, K.Y.; Armstrong, C.G.; Price, M.A.; Lamont, J.H.: A small feature suppression/unsuppression system for preparing b-rep models for analysis. In ACM Symposium on Solid and Physical Modeling and Applications, 113–124. Cambridge MA, United States, 2005. http://doi.org/10.1145/1060244.1060258.

[11] Nolan, D.C.; Tierney, C.M.; Armstrong, C.G.; Robinson, T.T.: Defining simulation intent. Computer-Aided Design, 59, 50–63, 2015. http://doi.org/10.1016/j.cad.2014.08.030.

[12] Nolan, D.C.; Tierney, C.M.; Armstrong, C.G.; Robinson, T.T.; Makem, J.E.: Automatic dimensional reduction and meshing of stiffened thin-wall structures. Engineering with Computers, 30(4), 698–701, 2014. http://doi.org/10.1007/s00366-013-0317-y.

[13] Price, M.A.; Armstrong, C.G.: Hexahedral mesh generation by medial surface subdivision: Part 1 solids with convex edges. International Journal for Numerical Methods in Engineering, 38, 3335–3359, 1995. http://doi.org/10.1002/nme.1620381910.

[14] Provasi, R.; de Arruda Martins, C.: A finite macro-element for orthotropic cylindrical layer modeling. Journal of Offshore Mechanics and Arctic Engineering, 135(3), 031401–031401–9, 2013. http://doi.org/10.1115/1.4023793.

[15] Suzuki, S.; Abe, K.: Topological structural analysis of digitized binary images by border following. Computer Vision, Graphics, and Image Processing, 30(1), 32–46, 1985. http://doi.org/10.1016/0734-189X(85)90016-7.

[16] Thakur, A.; Banerjee, A.G.; Gupta, R.K.: A survey of cad model simplification techniques for physics-based simulation applications. Computer-Aided Design, 41(2), 64–80, 2009. http://doi.org/10.1016/j.cad.2008.11.009.

[17] Yildiz, Y.; et al.: Development of a feature based CAM system for rotational parts. Gazi University Journal of Science, 19, 35–10, 2006.